Supporting Information

Preparation of Menthol-Based Hydrophobic Deep Eutectic Solvents for Extraction of Triphenylmethane Dyes: Quantitative Properties and Extraction Mechanism

Taotao Fan[a], Zongcheng Yan[a], Chanyuan Yang[a], Shunguo Qiu[a], Xiong Peng[a], Jianwei Zhang[a], Lihua Hu[a], Li Chen[a,*]

[a] School of Chemistry and Chemical Engineering, South China University of Technology, Guangzhou 510640, China

[*]Corresponding author. E-mail: celichen@scut.edu.cn (Li Chen)

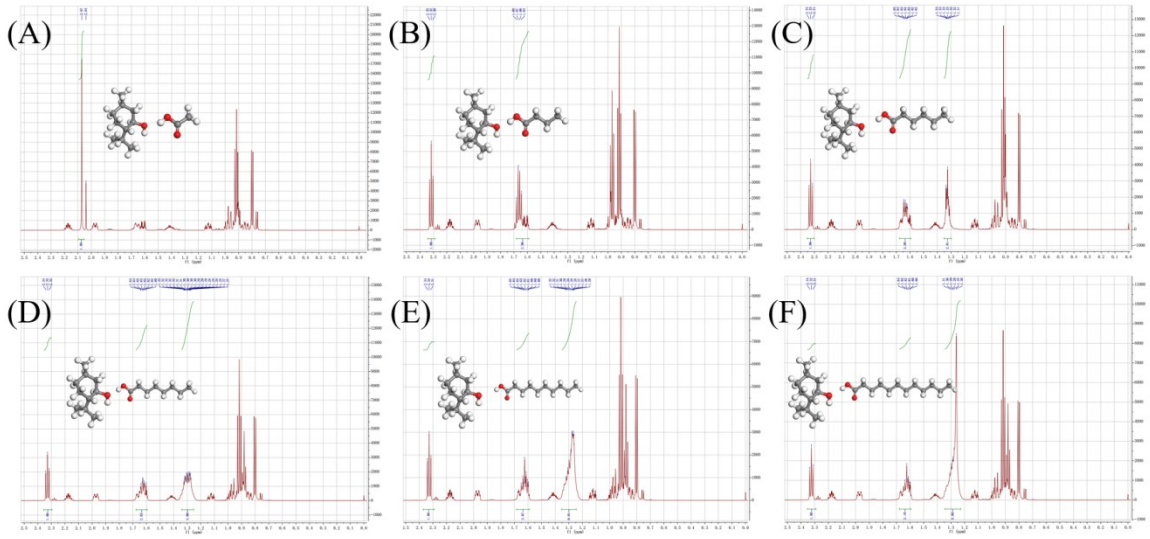

Fig. S1. 1H NMR spectra of DESs: (A) M-C_2 (molar ratio of 1:1, in $CDCl_3$), (B) M-C_4 (molar ratio of 1:1, in $CDCl_3$), (C) M-C_6 (molar ratio of 1:1, in $CDCl_3$), (D) M-C_8 (molar ratio of 1:1, in $CDCl_3$), (E) M-C_{10} (molar ratio of 1:1, in $CDCl_3$), and (F) M-C_{12} (molar ratio of 1:1, in $CDCl_3$).

Table S1. Other methods for dye removal and their extraction capabilities reported in the previous literature. (C_{ini} = initial concentration of dye)

Materials	Target Analyte	Methods	Experimental conditions	C_{int}	Extraction capacity or efficiency	Ref.
MHNTs@C_{16}mimBr	Methyl red; Methyl orange;	[a]MHMSPE-HPLC	12 mg C_{16}mimBr 60 mg MHNTs Time = 5 min;	10 mg/l	121.95 mg/g 196.08 mg/g	1
[b]Magnetic CFG	Rhodamine B; Methylene Blue; Congo red; Methyl green;	Adsorption	250 mg/l CFG; Time = 30 min;	0.01 mM	121.8 mg/g; 93.5 mg/g; 104.5 mg/g; 88.3 mg/g;	2
Inonotus dryadeus Fungi	Methylene Blue	Bio-adsorption	5 mg dry Inonotus dryadeus	60 mg/l	137 mg/g; 93.2%	3
Titanate nanotubes	Methylene blue	Adsorption	20 mg calcined titanate nanotubes; Time = 120 min	50 mg/l	133.33 mg/g	4
[c]HNT–Fe_3O_4	Methylene Blue; Neutral red; Methyl orange	Adsorption	2 g/l of HNT–Fe_3O_4; Time = 18 h	0.1 mmol/l	18.49 mg/g; 13.62 mg/g; 0.7 mg/g;	5
Zeolite	Methylene blue	Adsorption	6 g/l Zeolite; pH = 7; Time = 480 min;	30 mg/l	16.37 mg/g	6
[d]PTS-PPy NFsM	Auramine O; Chrysoidine; Rhodamine B;	Micro-solid phase extraction (HPLC-DAD)	Circular NFsM (0.5cm Diameter); 1% NaCl;	0.5 mg/l	3.25 mg/g; 9.95 mg/g; 8.05 mg/g	7
MnBi alloy powders	Congo red	Degradation	Time = 20min; 50℃; 2 mg/l $CuCr_2O_4$;	40 mg/l	95%	8
$CuCr_2O_4$	Tartrazine	Photocatalytic	125 W high-pressure mercury lamp (200-600 nm); Time = 120 min	50 mg/l	99.6%	9

Mesoporous KIT-5-gC_3N_4	Methylene blue	Photocatalytic	0.3 mg/ml Mesoporous KIT-5-gC_3N_4; visible light; Time = 60 min	5 mg/l	85.5%	[10]
Pa-AgNps	Blue CP Yellow 3RS	Photocatalytic	50 µg/ml Pa-AgNPs; Sunlight; Time = 30 min	50 mg/l	90% 83%	[11]
AgNP	Methylene blue	Photocatalytic	Direct sunlight (787 ± 25 Wm^{-2}); Time = 173 min	40 mg/l	98.04%	[12]
Ternary ZnCdSO	Methylene blue Rhodamine B	Photocatalytic	400 W metal halide lamp; 833.3 mg/l ZnCdSO; Time = 120 min	0.33 mg/l	95.26% 75.25%	[13]
$Bi/SbSnO_2$ ceramic membranes	direct orange S	Electrocatalysis	Voltage 1V; 0.4 MPa;	40 mg/l	99%	[14]
EC-Cu-PDS	Acid Orange 7	Electrocatalysis	j =1 mA cm^{-2}; PDS = 4 mM; Cu^{2+} = 1 mM, H_2PO_4/HPO_4 = 10mM;	0.1 mM	70%	[15]
TiO_2/OCF	Brilliant Green	Photoelectrocatalysis	j = 10 mA cm^{-2}; 4.4 cm^2; 0.1 mol/l K_2SO_4; Time = 300 min;	100 mg/l	85%	[16]
[e]SS/PbO_2	Amaranth	Electrocatalysis	j = 25 mA.cm^{-2}; 4 cm^2; 0.1 M H_2SO_4; Time = 300 min;	0.015 m M	70%	[17]
$TiRuSnO_2$	Methyl Orange	Electrocatalysis	j = 0.5 A; 50 cm^2； 0.05 M Na_2SO_4; Time = 20 min	100 mg/l	69%	[18]
Au/TiO_2	Methyl Orange	Photoelectrocatalysis	j = 30 mA.cm^{-2}; 7.1 cm^2; 0.1 M Na_2SO_4	5.2 mg/l	68%	[19]
[f]MEUF	Reactive Black 5; Reactive Orange 16	Ultrafiltration	1g/l Cetylpyridinium chloride; Time = 60min	50 mg/l	99.7% 99.6%	[20]
[g]O_3/TiO_2/AC	Methylene blue	Ozone-based processes	Ozone generator(Input rate of 0.45 g/h); Time = 40 min	100 mg/l	95.4%	[21]
Macroalgae Chara sp.	Malachite Green	Biological treatments	4g algal biomass;	10 mg/l	92.75%	[22]
Iron electrodes	Acid yellow 36	Electrocoagulation	0.4 g/l NaCl;	50 mg/l	85%	[23]

[a]MHMSPE: mixed hemimicelles magnetic solid phase extraction

[b]CFG: $CoFe_2O_4$/reduced graphene oxide (rGO)

[c]HNT: halloysite nanotube

[d]PTS-PPy NFsM: P-Toluene sulfonate (PTS^-) - doped polypyrrole (PPy) functionalized nanofibers mat

[e]SS/PbO_2: Stainless steel/PbO_2

[f]MEUF: Micellar-enhanced ultrafiltration

[g]O_3/TiO_2/AC: ozone/activated carbon (O_3/AC) and ozone/TiO_2/activated carbon

The Preparation process of the materials in Table S1:

MHNTs@C_{16}mimBr: A known amount of halloysite powder was suspended in 150 ml of deionized water and the mixture was sonicated for 15 min, and then the quantity of $FeCl_3.6H_2O$ and $FeSO_4.7H_2O$ were added. The mixture was stirred for 10 min at 60 °C in the N_2 atmosphere. Subsequently, 100 ml (25%) of ammonia solution was added drop wise into the mixture solution. The addition of the base to the Fe^{2+}/Fe^{3+} salt solution resulted in the immediate formation of black precipitates of MHNTs. Then, the resulting reaction mixture was aged for 4 h at 60 °C. The MHNTs were separated using an external magnetic field and washed several times sequentially with water and ethanol till pH = 7. Finally, the MHNTs were dried in a vacuum at 60 °C[1].

Magnetic CFG: CFG nanocomposites were synthesized via a solvothermal process described as follows. Typically, 40 mg of GO was dispersed in a 20 ml of ethylene glycol and DIW cosolvent (v/v = 3 : 1) with sonication for 2 h. At the same time, 135 mg of $FeCl_3{\cdot}6H_2O$ (0.5 mmol) and 59.5 mg of $CoCl_2{\cdot}6H_2O$ (0.25 mmol) were dissolved in 15 ml of DIW. After the GO dispersion was added, the resulting solution was stirred at room temperature for 5 h for the ion exchange. Then, $N_2H_4{\cdot}H_2O$ (3 ml), which acted as both reducing agent and mineralizer, was added into the GO solution and the mixture was stirred for 0.5 h. The mixture was then transferred to a 50 ml Teflon-lined stainless steel autoclave and heated at 180 °C for 12 h. The product was collected, washed with DIW and absolute ethanol several times, and finally dried at 60 °C for 5 h[2].

Inonotus dryadeus Fungi: Isolation of Inonotus dryadeus Fungi from Natural Source. The orange brownish and spongy fungi grow on stipule of the tree during rainy season, which becoming dark on drying; exuding amber-colored droplets when young, through its pores. Fungi sample was collected from stipule of the Delonix regia tree in and around University of Pune campus. It was then squeezed to get an extract and the fungi were observed to change color

from yellowish orange to dark brown as soon as extract was taken out. When it was kept in a beaker for 20 minutes, this liquid forms two layers; a black brown substance settled down, while a supernatant and completely transparent lemon colored liquid stays above. The supernatant did not show adsorption/separation of MB. The brown sediment at the bottom of the beaker was harvested and dried in hot air oven for 6 hours at 70°C.

Titanate nanotubes: In a typical synthesis, 0.3 g of Degussa P25 was added into a 10 M NaOH aqueous solution. After stirring for 24 h, the specimen was transferred into a sealed Teflon container statically heated at 130 °C for 72 h. Then the product was centrifugally separated at 4000 rpm and washed with ethanol at room temperature until the pH value of the supernatant dropped to about 7. The resulting powder was further dried at 80 °C for about 4 h in air. Finally, the samples were calcined at 400 °C in air for 2 h and CTNTs were obtained[4].

HNT–Fe_3O_4: The HNT–Fe_3O_4 were prepared from a suspension of 0.5 g HNT in a 200 ml solution of 1.165 g $FeCl_3 \cdot 6H_2O$ and 0.6 g $FeSO_4 \cdot 7H_2O$ at 60 °C under N_2. NH_3H_2O solution (20 ml, 8 mol/l) was added dropwise to prepare iron oxides. The pH of the final mixtures was controlled in the range of 9–10. The mixtures were aged at 70 °C for 4 h and then washed 3 times with distilled water. The obtained composites were dried at 100 °C for 3 h[5].

Zeolite: the zeolite was crushed and sieved through mesh screens, and a fraction of the particles of average size (40–60 mesh) was soaked in tap water for 24 h, rinsed with distilled water. After drying at 373 K in an oven, the sample was stored[6].

PTS-PPy NFsM: Briefly, 100 μm of thick PAN NFsM was first fabricated by electrospinning. Then, the PAN NFsM (10 cm × 10 cm) was immersed in pyrrole monomer solution (0.1 mol/l) for 1 h. Afterward, the polymerization of pyrrole and the deposition of PPy on the white PAN nanofibers were initiated by the addition of ferric chloride hexahydrate ($FeCl_3 \cdot 6H_2O$) solution (molar ratio of Py:$FeCl_3$, 1:1) into above solution and incubation for 12 h at 25 °C. The total reaction volume was 100 ml. Finally, this resultant black PPy NFsM with Cl^- as a dopant was formed and subsequently washed with anhydrous ethanol and deionized water repeatedly until the solution turned colorless, and then air-dried. For the synthesis of PTS^- doped PPy NFsM (namely as PTS-PPy NFsM), pyrrole monomer solution (0.1 mol/l) was replaced by sodium p-toluene sulfonate (NaPTS) (0.1 mol/l) and pyrrole monomer (0.1 mol/l) mixed solution, the remaining steps were the same as described above. The PPy hollow NFsM was prepared by soaking the PPy NFsM in dimethylformamide for 12 h to remove the PAN fiber cores. This generated PPy hollow NFsM was then washed with deionized water and air-dried[7].

MnBi alloy powders: $Mn_{55}Bi_{45}$ alloy ingot, with the nominal compositions, was prepared by induction melting in a high-purity argon atmosphere, using mixtures of the Mn (99.99 mass %), and Bi (99.99 mass %) elemental plates. Heat treatments were carried out at 290 °C for 24 h with a heating rate of 5 °C/min in a vacuum tube furnace with a pressure of 10−3 Pa and followed by cooling in the furnace. The annealed ingots were crushed and grounded into powders, and sieved using #1000 mesh (resulting in particles with average sizes of 13 μm). The MnBi powders were milled with low-energy ball milling process at room temperature. The milling was performed in ethanol with zirconia balls (3 mm in diameter) and the ball-to-powders weight ratio was about 10:1. The powders were milled for 30 h with a milling speed of 100 rpm[8].

$CuCr_2O_4$: For the synthesis, 10 mmol $Cu(NO_3)_2.3H_2O$ (98 %, Vetec), 20 mmol $Cr(NO_3)_3.9H_2O$ (98 %, Vetec) and 30 mmol urea (99 %, Dinâmica) were dissolved in 60 ml of ultrapure water. The solution was left under magnetic stirring for 1 h at 90 °C for homogenization. After this step, the temperature was raised to 100 °C until complete elimination of the water and formation of a gel. The gel was then transferred to a muffle oven at 300 °C where it remained until the auto-ignition process was completed which led to the formation of the ceramic powder. Finally, the powder was calcined at 600 °C for 3 h to yield $CuCr_2O_4$[9].

Mesoporous KIT-5-gC_3N_4: The large pore cage type mesoporous silica, named KIT-5 was prepared in aqueous solution using pluronic F127 template as a non-ionic structure directing agent and tetraethylorthosilicate (TEOS) as silica precursor. In a typical synthesis of KIT-5, 2.5 g of pluronic F127 was dissolved in 120 ml of distilled water containing 5.25 ml of concentrated hydrochloric acid (35 wt% HCl). To this mixture, 12 g of TEOS was added. The mixture was stirred at 45 °C for 24 h for the formation of mesostructured product. After 24 h, the reaction mixture was kept in a Teflon lined autoclave and heated for 24 h at 150 °C. The solid product was then filtered, washed with deionized water and dried at 80° C. Finally, the sample were calcined at 550° C for 6 h in order to remove the template. g-C_3N_4 nanoparticles was synthesized by thermal treatment of melamine which is used as precursor. 4 g (3.1 M) of melamine was taken in a ceramic crucible with a lid, and then placed in a muffle furnace and calcined at 500 °C at a heating rate of 2 °C/min for 4 h. The resulting yellowish g- C_3N_4 nanoparticles were gathered for further use. 1 g of mesoporous KIT-5 and 0.5 g of g- C_3N_4 nanoparticles were allowed to stir in 80 ml of double distilled water in a 250 ml beaker. To this solution 20 mg of H_2BDC and 30 mg of TCA were added as acid modulators and were allowed to stir for 2 h under room temperature. Then the solution was kept in a Teflon lined autoclave for 24 h for hydrothermal

treatment and then cooled to room temperature. After cooling, the resultant mixture was centrifuged, washed, filtered using Whatman grade filter paper and dried at 40 °C to get KIT-5 functionalized with g-C_3N_4 nanoparticles[10].

Pa-AgNps: Fresh leaves of C. papaya were collected from IIT Delhi campus. After collection, leaves were cleaned using double distilled water. 10 g of properly washed leaves (using distilled water) were chopped into small pieces; these chopped leaves were then boiled with 100 ml distilled water for 10 min at 60 °C. Further, the boiled mixture was cooled for 30 min and the leaf extract was obtained after filtration through Whatman No. 1 filter paper[11].

AgNP: In a typical synthesis protocol, the desired concentration of $AgNO_3$ solution (5 ml) was slowly introduced into 45 ml of the pineapple extract with constant stirring at room temperature under dark conditions. To study the effect of pH, synthesis of AgNPs was conducted adjusting pH of pineapple waste extract to 4, 6, 8 and 10. The reduction capacity of pineapple waste extract to synthesize silver nanoparticles was evaluated where five different concentrations of $AgNO_3$ were introduced in the PW extract with 1:9 ratio (v/v) such that the final Ag conc. in resulting mixture was obtained as 0.5, 1.0, 1.5, 5, and 9 mM[12].

Ternary ZnCdSO: ZnO–CdS–CdO composite samples were prepared by a simple co-precipitation method followed by calcination. At the beginning 0.5 M zinc acetate dihydrate was dissolved into 25 ml D.I. water, then potassium hydroxide solution was prepared using 2 M KOH dissolved in 25 ml D.I. water and two solutions were mixed together via continuous magnetic stirring. Subsequently, 0.1 mmol cadmium chloride monohydrate solution was prepared with 10 ml of D.I. water added to the above suspension. 4 ml of ethylenediamine and 4 ml polyethylene glycol 400 was then added to it. 10 ml of 0.1 mmol sodium sulphide nonahydrate D.I. water solution was added to this mixture dropwise and the total suspension was kept at 100 °C temperature for 2 h. Different samples were prepared by varying the equimolar concentrations of cadmium chloride monohydrate and sodium sulphide nonahydrate, e.g., by 0.1, 0.5, 1 mmol. Finally, a yellow colour precipitate was obtained and washed by centrifugation several times with water and ethanol. The final product was dried for 5 h at 80 °C temperature, followed by calcination at 300 °C temperature for 3 h. The pristine sample was named as ZnO, while the composites were labelled as ZnCdSO-0.1, ZnCdSO-0.5 and ZnCdSO-1, according to the molarity of equi-molar cadmium chloride monohydrate and sodium sulphide nonahydrate components incorporated in the mixture[13].

Bi/$SbSnO_2$ ceramic membranes: The Bi/$SbSnO_2$ composites were synthesized via a sol-gel method. The typical procedure was as follows: 2 ml of concentrated hydrochloric acid, 50 ml of absolute ethanol and 3 ml of deionized

water were added to 12.12 g of SnO_2 with magnetic stirring for 36 h at 25 °C to obtain a SnO_2 sol. Subsequently, 1.84 g of $SbCl_3$ was added to the SnO_2 sol with a magnetic stirrer for 6 h at 25 °C to obtain the $SbSnO_2$ sol. Next, 10 ml of absolute ethanol and 2 ml of deionized water were added to 0.318 g of $Bi(NO_3)_3$ with a magnetic stirrer for 3 h at 25 °C to obtain the $Bi(NO_3)_3$ solution. Finally, the $Bi(NO_3)_3$ solution was slowly trickled into the $SbSnO_2$ sol with magnetic stirring at 1 ml/min for 2 h at 40 °C to obtain Bi/Sb co-doped SnO_2 sol. The mole ratio of Bi, Sb and SnO_2 was nearly 1:10:100 in the Bi/$SbSnO_2$ sol; the results were satisfactory[14].

EC-Cu-PDS: The test solutions consisted of AO7 with initial concentration of 0.1 mM. To this was added 1 mM of metallic salt, being either iron(II) sulfate, copper(II) sulfate, cobalt(II) chloride or silver(I) nitrate along with 4 mM of either potassium persulfate (PDS) or potassium peroxymonosulfate (PMS, commonly known as Oxone™). The solution was buffered with 10 mM phosphate (K_2HPO_4/KH_2PO_4), with sulfuric acid or sodium hydroxide used to adjust to the required pH of 2, 3, 7 or 10. Batch experiments were carried out in an undivided three electrode electrochemical cell containing 100 ml of electrolyte. Carbon cloth (2225 Type 900 Activated Carbon Fabric, Spectracarb) of dimensions of 1 × 1 cm, unless otherwise stated, was used as both the working and counter electrodes. Carbon cloth was chosen as it is inert, has a large overpotential for water splitting and is cheaper than other carbon-based electrodes. The reference electrode was a saturated calomel electrode (+0.241 V vs SHE, CH Instrument), but all potentials reported have been converted to the standard hydrogen electrode (SHE) scale. The experiments were performed in duplicate with errors within 5%[15].

TiO_2/OCF: CF samples were produced from polyacrylonitrile (PAN) precursor. The fibers were oxidized at 200 °C and submitted to heat treatment temperature of 1000 °C. CF samples were cut with dimension of 1 cm^2. Electrochemical oxidative treatment (EOT) and TiO_2 electrodeposition were performed at room temperature using Autolab-Pgstat 302 equipment and a conventional three-electrode glass cell with quartz window, with platinum wire and Ag/AgCl/KCl(sat) as counter and reference electrode, respectively. The EOT was performed on CF surface applying fixed potential of 2.0 V vs Ag/AgCl/KCl(sat) for 5, 10, 20, and 30 min in 0.5 mol/l H_2SO_4. The TiO_2 electrodeposition on CF substrates was performed under potentiostatic mode at a fixed potential of 0.75 V vs Ag/AgCl/KCl(sat) for 30 min deposition in a 5 mmol l^{-1} $TiCl_3$ (pH = 2) + 0.1 mol/l KCl aqueous solution. Subsequently, to improve the TiO_2 crystallinity, the composites with optimized conditions were heat-treated (HT) at 500 °C with a ramp rate of 10 °C/min for 2, 3 and 4 h in an argon atmosphere[16].

Stainless steel (SS)/PbO_2: Stainless steel plates (AISI 304 (Fe/Cr18/Ni10) were used as electrode substrates. Before the SiOx deposition, the stainless steel substrates were cleaned with 2-Propanol and acetone in ultrasonic bath (Ultrasonic Batch-FALC) for 20 min, respectively, to remove any surface contamination. The PbO_2 layer was deposited on AISI 304 substrate by the electrochemical deposition process. In this step, the deposited PbO_2 was synthesized in situ from a 0.5 M $Pb(NO_3)_2$ + 0.5 M HNO_3 solution. Electrodeposition was performed at 25 °C under a constant anodic current density (j = 30 mA cm^{-2}) for 17 min[17].

TiRuSnO_2: The Ti–Ru–Sn ternary oxide anodes, hereafter indicated as TiRuSnO_2, have been prepared by coating titanium sheet by thermal decomposition of $TiCl_4$, $RuCl_3 \cdot 3H_2O$ and $SnCl_4 \cdot 5H_2O$ isopropanol solution. The titanium plate with a thickness of 1.5 mm was sandblasted chemical etched in hydrochloric concentrated acid. The solution of the precursor was painted on the titanium and the solvent was evaporated in air at 80 °C. Then the sheets were fired at 450 °C for 1 h. Thereafter, this procedure was repeated until the coating thickness was 50 μm. The nominal composition of the ternary oxide was $Ti/Ti_{0.5}Ru_{0.45}Sn_{0.05}O_2$[18].

Au/TiO_2: The Au/TiO_2 hybrid structures were constructed on the Ti wires using electrochemical methods. First, the TiO_2 nanotube array layer was prepared with anodization of the Ti wire. The Ti wires with a diameter of 1.5 mm and a length of 6 cm were used as the anode. Au nanoparticles were electrodeposited on TiO_2 nanotubes using 0.02 mM hydrogen tetrachloroaurate solution via a multi-potential step technology[19].

Micellar-enhanced ultrafiltration (MEUF): A GN polymeric membrane of molecular weight cut-off 10,000, obtained from Osmonics, was used for the experiments. The permeability of the membrane was 6.28×10^{-11} m/Pa.s. Three hundred ml stirred cell (Sterlitech), model Sterlitech™ HP4750, USA, was used to conduct unstirred dead-end filtration experiments. The membrane diameter was 49 mm and the effective membrane area was 14.6 cm^2. The maximum operating pressure was 1000 psig (69 bar)[19].

O_3/TiO_2/AC: TiO_2/AC catalyst was prepared by the sol–gel method. Precursor solutions for TiO_2/AC catalyst were prepared as follows: 7.50 ml tetrabutylorthotitanate was dissolved in 20 ml ethanol. The solution was stirred vigorously followed by addition of 10 ml ethanol solution containing 0.75 ml acetic acid, 1.00 ml distilled water and 1.00 ml nitric acid. When this reaction ended, methanol solution containing 1.00 g polyethyleneglycol was added. Then, 5.00 g of prepared AC was added into the solution, dipping for 24 h, followed by filtration. The sample was firstly dried at 120 °C for 2 h and then baking at 450 °C for 2 h[21].

Iron electrodes: The electrocoagulation unit consisted of an 250 ml electrochemical reactor with iron (ST 37-2) anode and cathode. The electrodes were 30mm×50mm and interelectrodes distance was 2.5cm. The current density was maintained constant by means of a precision DC power supply (ADAK-PS 808)[23].

Table S2. Toxicity Classification According to Hodge and Sterner (1943)[24].

Toxicity class	Characteristic	LD50 (mg/kg) (Oral)
1	Extreme toxicity	<1
2	High toxicity	1-50
3	Moderate toxicity	50-500
4	Low toxicity	500-5000
5	Practically nontoxic	5000-15000
6	Relatively harmless	>15000

Table S3. Comparison table of the corresponding toxicity of DES components and comparative substances (Refer to LD50 experiment)

Substances	Animal species	Experimental method	Dose (mg/Kg)	References
Menthol	Rat	LD50, Oral	3180	[25]
Acetic acid	Rat	LD50, Oral	3310	[26]
Butyric acid	Rat	LD50, Oral	8790	[27]
Hexanoic acid	Rat	LD50, Oral	5970	[28]
n-octanoic acid	Rat	LD50, Oral	1410	[29]
Decanoic acid	Rat	LD50, Oral	3320	[30]
Lauric acid	Rat	LD50, Oral	12000	[29]
Ethanol	Rat	LD50, Oral	7000	[29]
Formaldehyde	Rat	LD50, Oral	100	[29]
Imidazole	Rat	LD50, Oral	220	[29]
Glycolic acid	Rat	LD50, Oral	1950	[29]
1,2-Dibromo-3-chloropropane	Rat	LD50, Oral	170	[31]
phenol	Rat	LD50, Oral	317	[32]
Dichloroethane	Rat	LD50, Oral	725	[29]
Sodium dodecyl benzene sulfonate	Rat	LD50, Oral	438	[33]
nicotine	Rat	LD50, Oral	188	[34]
ChCl-glycerol(1:3)	Rat	LD50, Oral	6400	[35]
ChCl-glycerol (1:2)	Rat	LD50, Oral	7733	[36]

The median lethal dose (LD50) means the minimum number of bacteria or toxins required to kill half of an animal of a certain weight or age through a specified infection route within a specified time. The unit is usually the ratio of the mass of the toxic substance to the weight of the experimental organism, such as "mg/kg". This indicator helps to compare the relative toxicity of different substances and estimate the toxic dose of the same substance between animals of different sizes to reveal the toxicity of the substance and whether the damage caused is reversible.

Table S4. GHS Hazard Statements of various components of DES and other common contrast substances

Substances	GHS Hazard Statements
Menthol	H315, H319
Acetic acid	H226, H314
Butyric acid	H314
Hexanoic acid	H311, H314, H318
n-octanoic acid	H314, H412
Decanoic acid	H315, H319, H412
Lauric acid	H315, H318, H319
Ethanol	H225
Formaldehyde	H301, H311, H314, H317, H331, H341, H350
Imidazole	H302, H314
Glycolic acid	H302, H314, H318, H332
1,2-Dibromo-3-chloropropane	H301, H340, H350, H360F, H373, H412
phenol	H301, H311, H314, H331, H341, H373
Dichloroethane	H225, H302, H319, H335, H412
Sodium dodecyl benzene sulfonate	H302, H315, H318
nicotine	H300, H310, H330, H411

GHS (Globally Harmonized System of Classification and Labeling of Chemicals) Hazard Statements is a normative document published by the United Nations that guides countries in controlling chemical hazards and protecting human health and the environment. It clearly stipulates the hazard classification, packaging and labeling of chemicals. (https://pubchem.ncbi.nlm.nih.gov/)

H225: Highly Flammable liquid and vapor [Danger Flammable liquids]

H300: Fatal if swallowed [Danger Acute toxicity, oral]

H301: Toxic if swallowed [Danger Acute toxicity, oral]

H302: Harmful if swallowed [Warning Acute toxicity, oral]

H310: Fatal in contact with skin [Danger Acute toxicity, dermal]

H311: Toxic in contact with skin [Danger Acute toxicity, dermal]

H314: Causes severe skin burns and eye damage [Danger Skin corrosion/irritation]

H315: Causes skin irritation [Warning Skin corrosion/irritation]

H317: May cause an allergic skin reaction [Warning Sensitization, Skin]

H318: Causes serious eye damage [Danger Serious eye damage/eye irritation]

H319: Causes serious eye irritation [Warning Serious eye damage/eye irritation]

H330: Fatal if inhaled [Danger Acute toxicity, inhalation]

H331: Toxic if inhaled [Danger Acute toxicity, inhalation]

H332: Harmful if inhaled [Warning Acute toxicity, inhalation]

H335: May cause respiratory irritation [Warning Specific target organ toxicity, single exposure; Respiratory tract irritation]

H340: May cause genetic defects [Danger Germ cell mutagenicity]

H341: Suspected of causing genetic defects [Warning Germ cell mutagenicity]

H350: May cause cancer [Danger Carcinogenicity]

H360F ***: May damage fertility [Danger Reproductive toxicity]

H373 **: Causes damage to organs through prolonged or repeated exposure [Warning Specific target organ toxicity, repeated exposure]

H411: Toxic to aquatic life with long lasting effects [Hazardous to the aquatic environment, long-term hazard]

H412: Harmful to aquatic life with long lasting effects [Hazardous to the aquatic environment, long-term hazard]

At present, it is a pity that there is no direct specific toxicity data of DES. We carefully analyzed the toxicity of its components or similar structural molecules. Because DES is only connected by hydrogen bonds, it will be separated into individual components in organisms (especially in polar environments), so we indirectly analyzed the toxicity of DES by analyzing the toxicity of its hydrogen bond donors and hydrogen bond acceptors.

Regarding the question of whether the toxicity of DES is an addition between the components of DES, Ventura et al. did a study on the toxicity correlation between cholinium chloride-based DES and each component using Microtox toxicity test (Microbics Corporation, 1992) to evaluate the inhibition of the luminescence in the marine bacteria V. fischeri. The results show that the toxicity of DES is basically the same as or slightly higher than the toxicity of each component[37].

It can be seen from the table that the toxicity of the DES components used in this topic is low toxicity according to the toxicity classification table, and lauric acid is even non-toxic. As a comparison of toxicity, the table also lists the molecular toxicity of other extractants and other common molecules as a comparison of toxicity.

The DES components we selected are all natural, rich in sources, and widely used in human life. Menthol is extracted from pure natural peppermint or peppermint oil. When menthol is added to medicines and foods, it can be used as an enhancer of peppermint flavor. Butyric acid is a fatty acid occurring in the form of esters in animal fats and plant oils. hexanoic acid is found naturally in various plant and animal fats and oils, and it has a role as a human metabolite and a plant metabolite. Octanoic acid is found naturally in the milk of various mammals and is a minor component of coconut oil and palm kernel oil. It has a role as an antibacterial agent, a human metabolite and an Escherichia coli metabolite. Decanoic acid is often used to make esters for perfumes and fruit flavors and as an intermediate for food-grade additives. Lauric acid is naturally present in various animal and vegetable oils and is the main component of coconut oil and palm kernel oil, and can also be used as a food additive. Although lauric acid is slightly irritating to mucous membranes, its toxicity is very low, so it is used in many soaps and shampoos.

At the same time, these components are environmentally safe and easily degradable. In the Japanese MITI test, 100 mg/l of menthol reached 0% of its theoretical BOD within 4 weeks using 30 mg/L of activated sludge inoculum[38]. In addition, other reports indicate that DL-menthol is easily biodegradable[39]. At an initial concentration of 100 mg/L, n-butanoic acid displayed a 72% theoretical biological oxygen demand (BODT) after 5 hours when incubated with activated sludge[40, 41]. A 5-day theoretical BOD of 44% was observed for hexanoic acid in an aerobic screening test

using a sewage inoculum[42]. In Warburg respirometer tests using an activated sludge seed, octanoic acid, present at a concn of 500 ppm, reached 9.8, 20.4, and 32.8% of its theoretical oxygen demand after 6, 12, and 24 hours incubation, respectively[43]. An aerobic biodegradation screening study of decanoic acid, based on BOD measurements, using a sewage inoculum and an unknown decanoic acid concn, indicated 23% of its theoretical BOD over a period of 20 days[44]. The theoretical BOD of lauric acid per day was determined to be 6.1% with the activated sludge inoculum in the Warburg respirometer[45]. In activated sludge medium, TOC (Total Organic Carbon) of the lauric acid reduces by 100% within 100 hours[46].

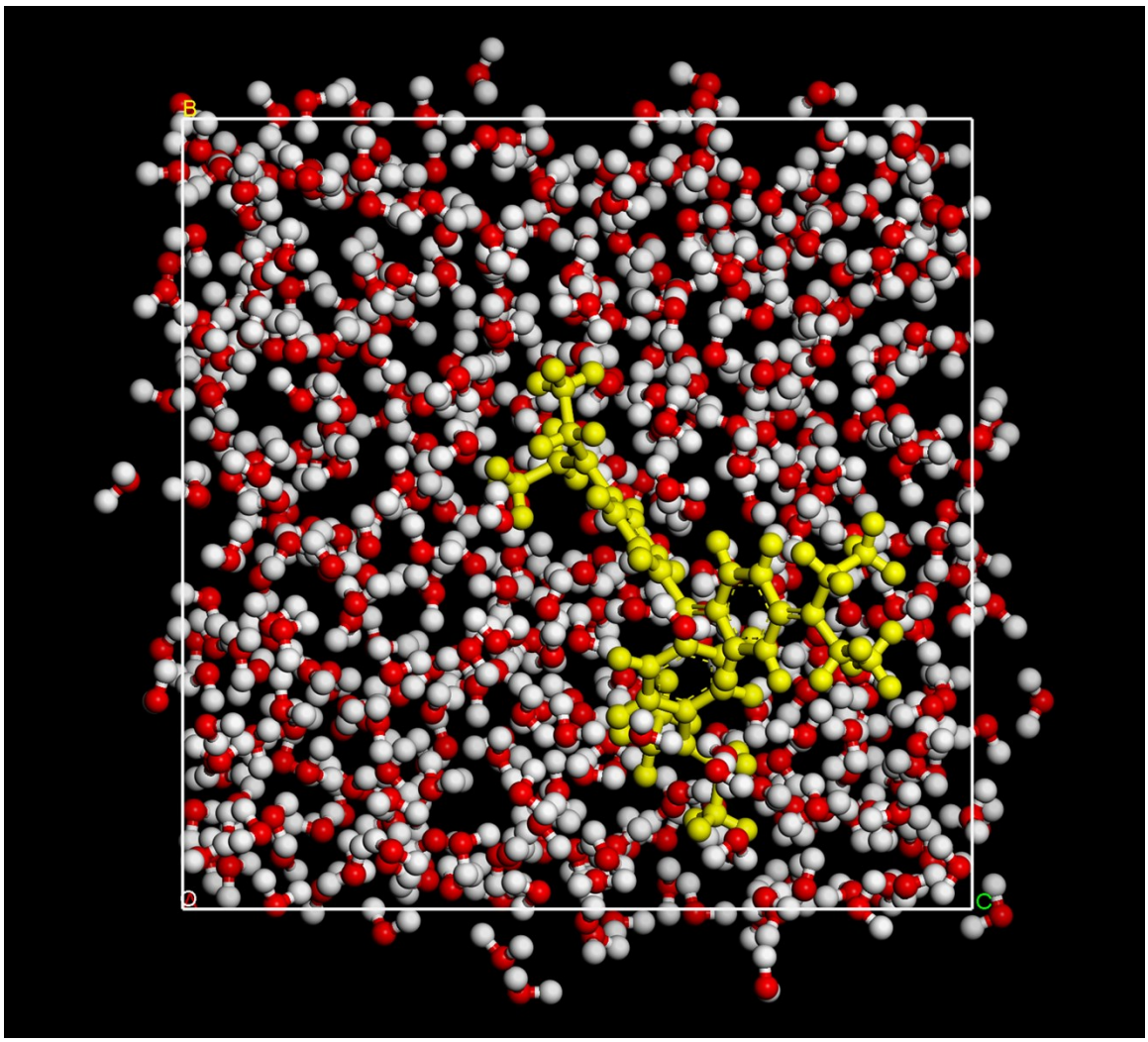

Fig. S2. Calculation of solvation free energy of EV in H_2O.

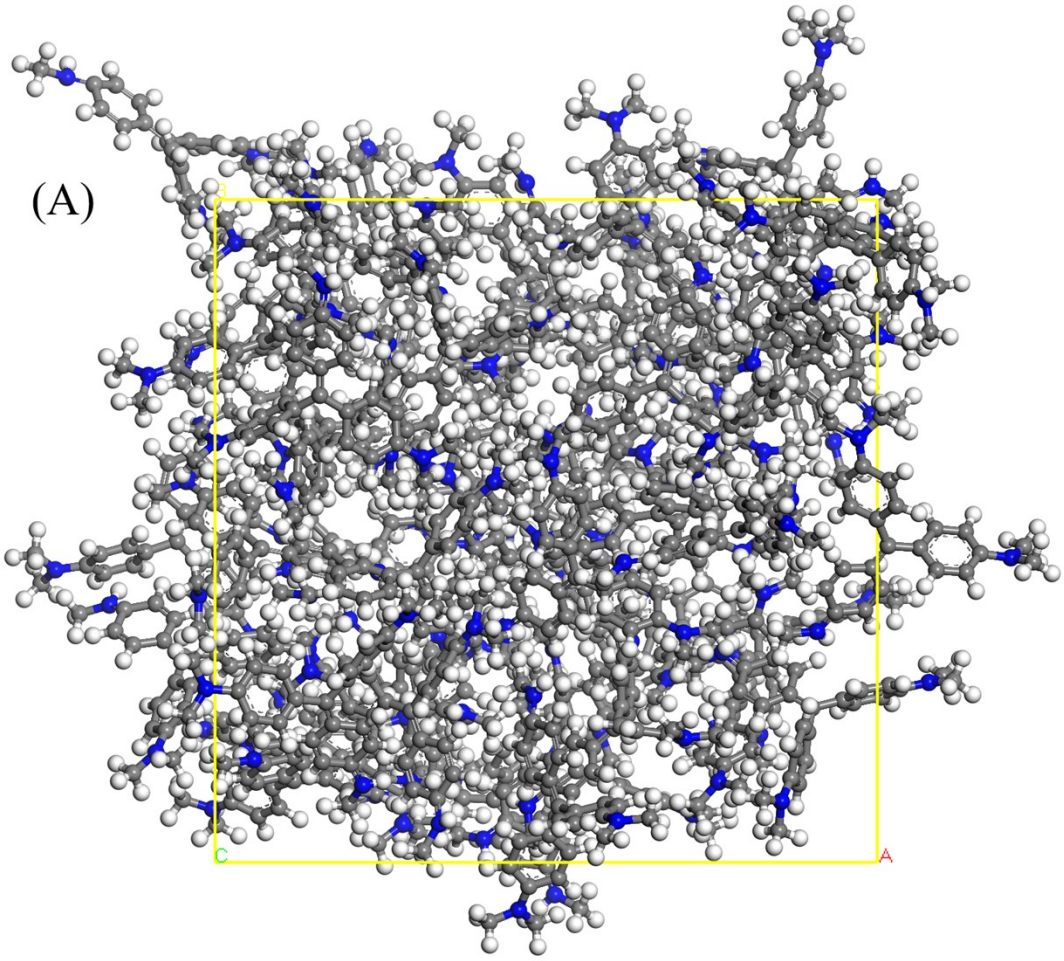

Fig. S3 (A). Cells of MV(A), CV(B), EV(C), C_{12}DES(D) and H_2O(E) and corresponding solubility parameters.

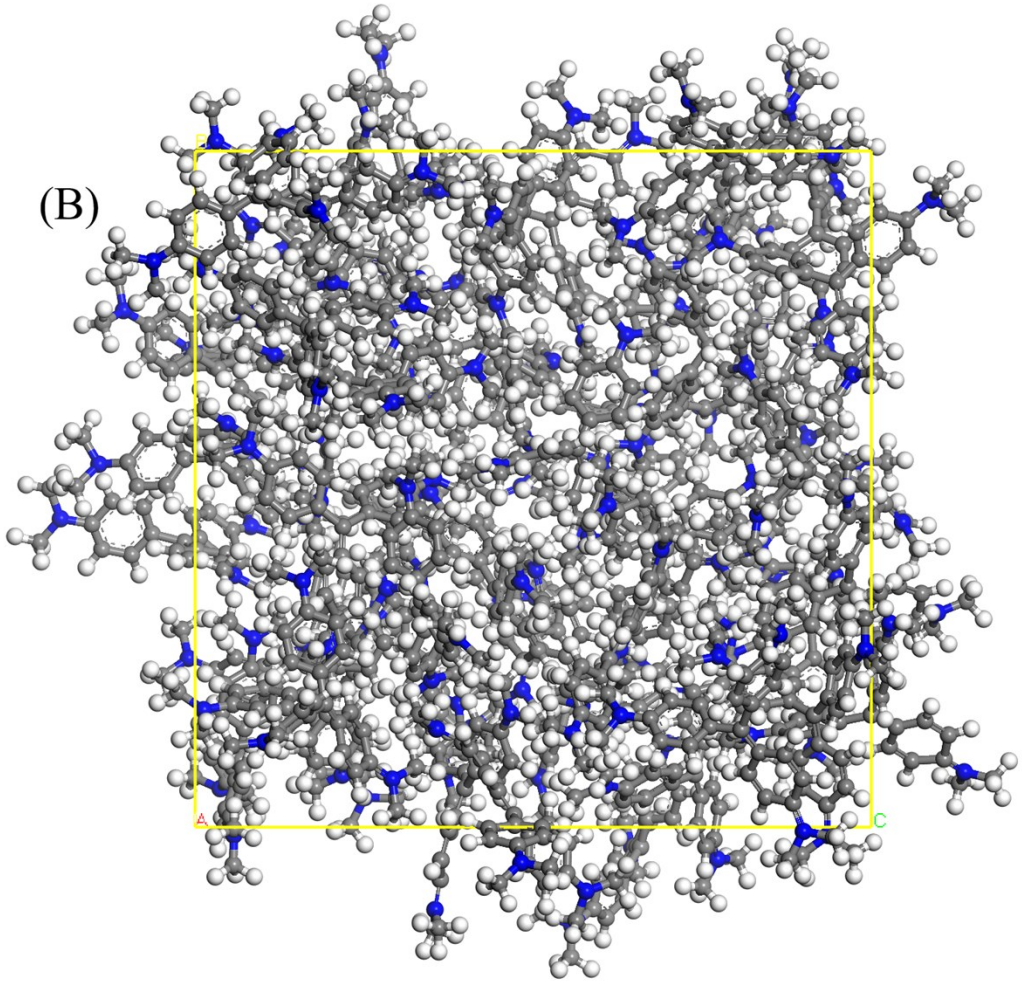

Fig. S3 (B). Cells of MV(A), CV(B), EV(C), C_{12}DES(D) and H_2O(E) and corresponding solubility parameters.

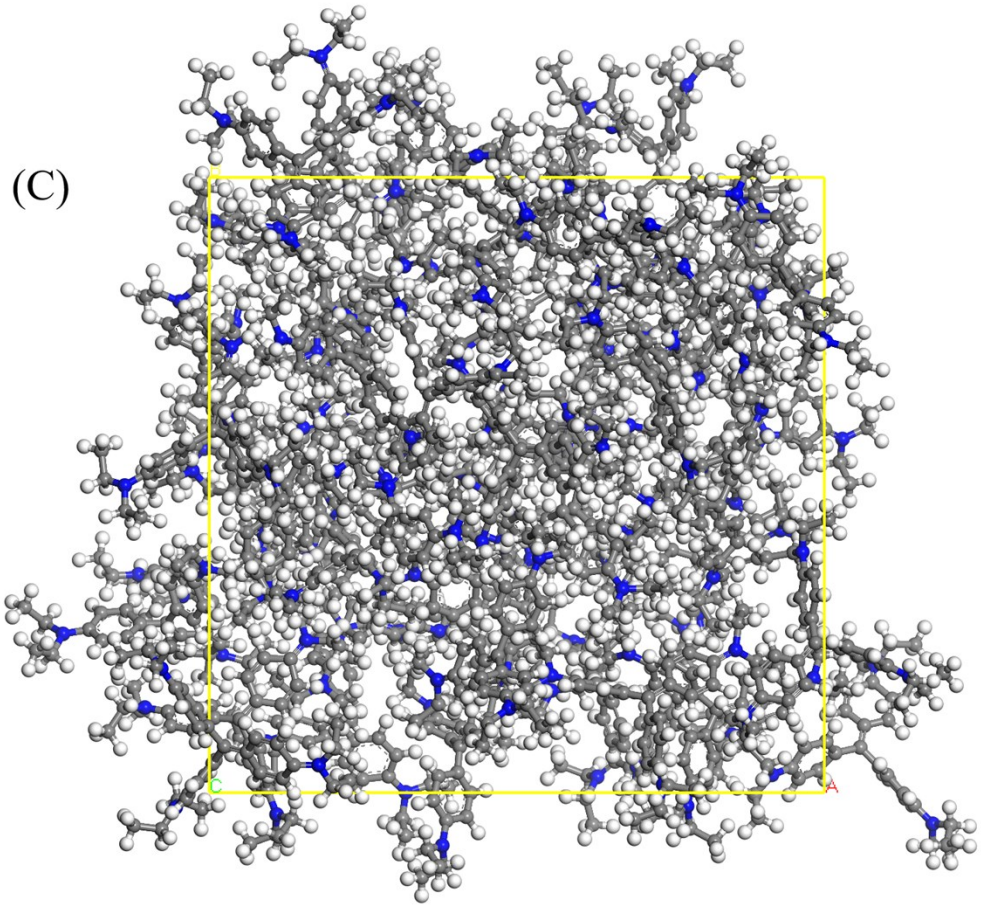

Fig. S3 (C). Cells of MV(A), CV(B), EV(C), C_{12}DES(D) and H_2O(E) and corresponding solubility parameters.

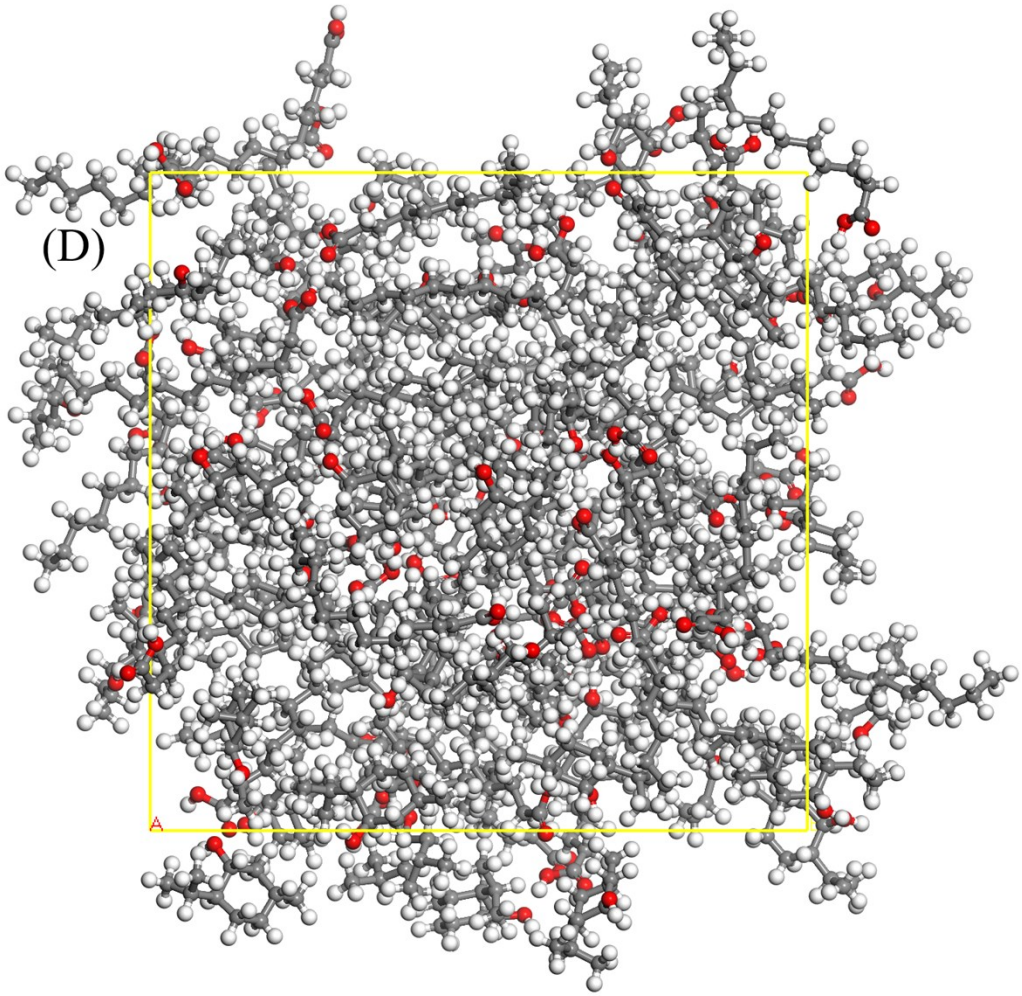

Fig. S3 (D). Cells of MV(A), CV(B), EV(C), C_{12}DES(D) and H_2O(E) and corresponding solubility parameters.

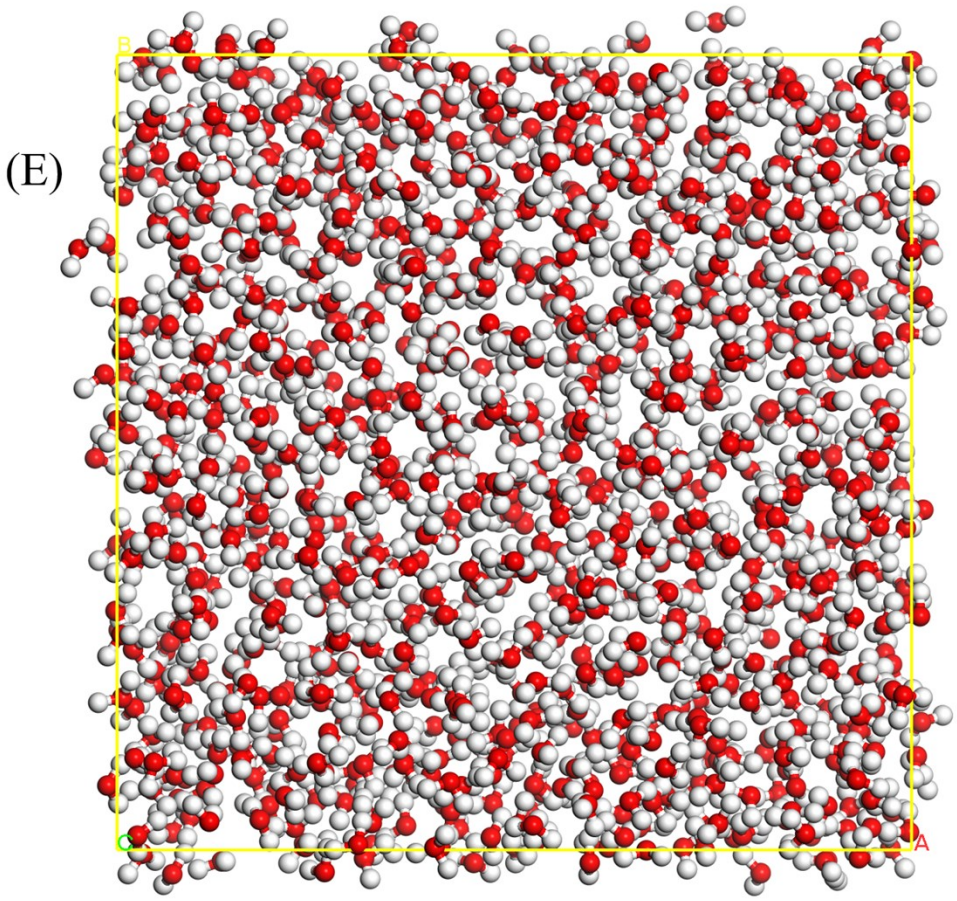

Fig. S3 (E). Cells of MV(A), CV(B), EV(C), C_{12}DES(D) and H_2O(E) and corresponding solubility parameters.

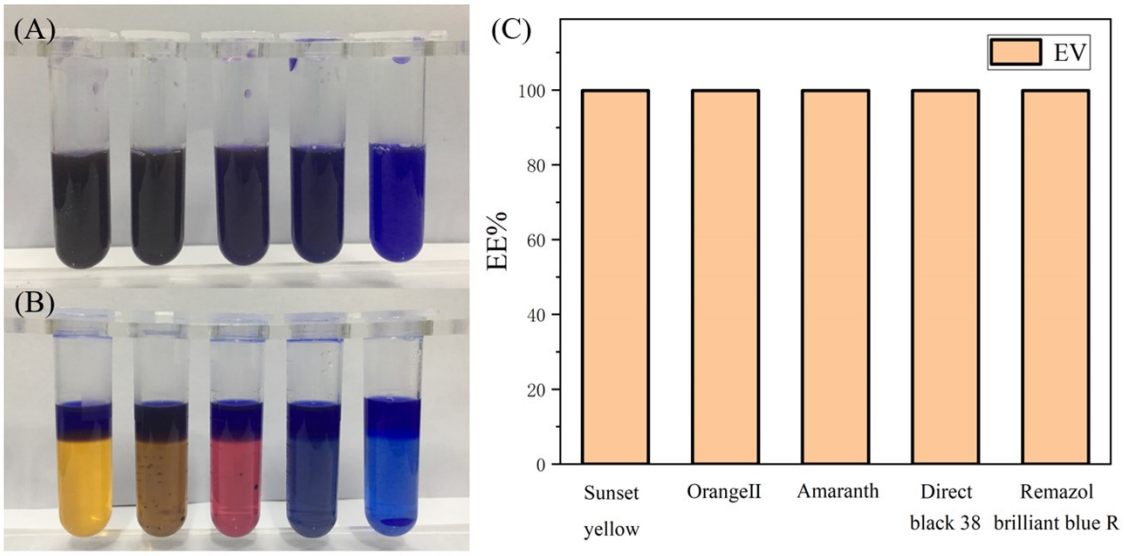

Fig. S4. (A) Mixed solvent of ethyl violet (EV) and different dye solvents (From left to right: Sunset Yellow, Orange II, Amaranth, Direct Black 38 and Remazol brilliant blue R). (B) The extraction effect diagram of the mixed dye after extraction by C_{12} DES (The sequence in the figure is as above). (C) The extraction efficiency of EV in five mixed dye solvents.

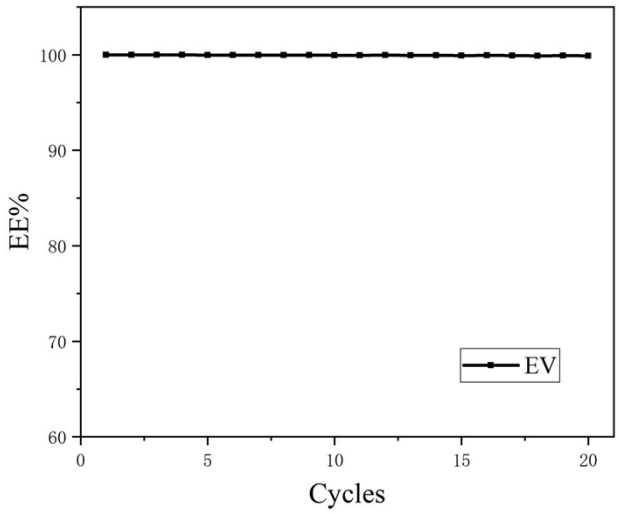

Fig. S5. The extraction efficiency curve of 20 cycles repeated extractions of EV using menthol based C_{12} DES.

References:

1 W. Liu, M. Fizir, F. Hu, A. Li, X. Hui, J. Zha and H. He, Mixed hemimicelle solid-phase extraction based on magnetic halloysite nanotubes and ionic liquids for the determination and extraction of azo dyes in environmental water samples, *J. Chromatogr. A*, 2018, **1551**, 10-20.

2 W. Yin, S. Hao and H. Cao, Solvothermal synthesis of magnetic CoFe2O4/rGO nanocomposites for highly efficient dye removal in wastewater, *RSC Adv.*, 2017, **7**, 4062-4069.

3 B. Ankamwar, Edible *Inonotus dryadeus* Fungi with Quick Separation of Water Pollutant Oils and Methylene Blue Dye, *ACS Biomaterials Science & Engineering*, 2016, **2**, 707-711.

4 L. Xiong, Y. Yang, J. Mai, W. Sun, C. Zhang, D. Wei, Q. Chen and J. Ni, Adsorption behavior of methylene blue onto titanate nanotubes, *Chem. Eng. J.*, 2010, **156**, 313-320.

5 Y. Xie, D. Qian, D. Wu and X. Ma, Magnetic halloysite nanotubes/iron oxide composites for the adsorption of dyes, *Chem. Eng. J.*, 2011, **168**, 959-963.

6 R. Han, J. Zhang, P. Han, Y. Wang, Z. Zhao and M. Tang, Study of equilibrium, kinetic and thermodynamic parameters about methylene blue adsorption onto natural zeolite, *Chem. Eng. J.*, 2009, **145**, 496-504.

7 F. Qi, L. Qian, J. Liu, X. Li, L. Lu and Q. Xu, A high-throughput nanofibers mat-based micro-solid phase extraction for the determination of cationic dyes in wastewater, *J. Chromatogr. A*, 2016, **1460**, 24-32.

8 X. Wang, B. Deng, L. Yu, E. Cui, Z. Xiang and W. Lu, Degradation of azo dyes Congo red by MnBi alloy powders: Performance, kinetics and mechanism, *Mater. Chem. Phys.*, 2020, **251**, 123096.

9 P. D. J. Cubas, A. W. Semkiw, F. C. Monteiro, P. Los Weinert, J. F. H. L. Monteiro and S. T. Fujiwara, Synthesis of $CuCr_2O_4$ by self-combustion method and photocatalytic activity in the degradation of Azo Dye with visible light, *Journal of Photochemistry and Photobiology A: Chemistry*, 2020, **401**, 112797.

10 D. N. Peter, R. Pushpakumar, E. Jayaseelan and N. Ananthi, Ordered cubic mesoporous KIT-5 functionalized with g-C3N4 nano particles for the complete discoloration and degradation of cationic dye, *Materials Today: Proceedings*, 2020.

11 A. Jain, F. Ahmad, D. Gola, A. Malik, N. Chauhan, P. Dey and P. K. Tyagi, Multi dye degradation and antibacterial potential of Papaya leaf derived silver nanoparticles, *Environmental Nanotechnology, Monitoring & Management*, 2020, **14**, 100337.

12 S. Agnihotri, D. Sillu, G. Sharma and R. K. Arya, Photocatalytic and antibacterial potential of silver nanoparticles derived from pineapple waste: process optimization and modeling kinetics for dye removal, *Applied Nanoscience*, 2018, **8**, 2077-2092.

13 D. Das and P. Nandi, Ternary ZnCdSO composite photocatalyst for efficient dye degradation under visible light retaining Z-scheme of migration pathways for the photogenerated charge carriers, *Sol. Energ. Mat. Sol. C.*, 2020, **217**, 110674.

14 Z. Wang, D. Ni, Y. Shang and Y. Guan, Recycling of dye from wastewater using a ceramic membrane modified with bismuth/stibium co-doped tin dioxide, *J. Clean. Prod.*, 2019, **213**, 192-198.

15 Z. T. How and D. J. Blackwood, Degradation of Acid Orange 7 through radical activation by electro-generated cuprous ions, *Journal of Environmental Chemical Engineering*, 2019, **7**, 103450.

16 L. A. Pereira, D. A. de Lima Almeida, A. B. Couto and N. G. Ferreira, Titanium dioxide/oxidized carbon fiber electrodes electrochemically produced and their influences on Brilliant Green dye degradation, *Mater. Res. Bull.*, 2020, **122**, 110642.

17 I. Elaissaoui, H. Akrout, S. Grassini, D. Fulginiti and L. Bousselmi, Effect of coating method on the structure and properties of a novel PbO_2 anode for electrochemical oxidation of Amaranth dye, *Chemosphere*, 2019, **217**, 26-34.

18 L. Labiadh, A. Barbucci, G. Cerisola, A. Gadri, S. Ammar and M. Panizza, Role of anode material on the electrochemical oxidation of methyl orange, *J. Solid State Electr.*, 2015, **19**, 3177-3183.

19 C. Fu, M. Li, H. Li, C. Li, X. G. Wu and B. Yang, Fabrication of Au nanoparticle/TiO2 hybrid films for photoelectrocatalytic degradation of methyl orange, *J. Alloy. Compd.*, 2017, **692**, 727-733.

20 A. L. Ahmad, S. W. Puasa and M. M. D. Zulkali, Micellar-enhanced ultrafiltration for removal of reactive dyes from an aqueous solution, *Desalination*, 2006, **191**, 153-161.

21 J. Zhang, K. Lee, L. Cui and T. Jeong, Degradation of methylene blue in aqueous solution by ozone-based processes, *J. Ind. Eng. Chem.*, 2009, **15**, 185-189.

22 A. R. Khataee, G. Dehghan, A. Ebadi, M. Zarei and M. Pourhassan, Biological treatment of a dye solution by Macroalgae Chara sp.: Effect of operational parameters, intermediates identification and artificial neural network modeling, *Bioresource Technol.*, 2010, **101**, 2252-2258.

23 M. K. R. M. M. Kashefialasl, Treatment of dye solution containing colored index acid yellow 36 by electrocoagulation using iron electrodes, *International Journal of Environment Science and Technology*, 2006, **2**, 365.

24 I. V. Berezovskaya, Classification of Substances with Respect to Acute Toxicity for Parenteral Administration, *Pharm. Chem. J.*, 2003, **37**, 139-141.

25 L. S. Clesceri, A. E. Greenberg and R. R. Trussell, *Standard Methods for Examination of Water and Wastewater*, Washington, DC: American Public Health Association, 1989.

26 MSDSonline, Editon edn., 2001, p. MSDSonline, a VelocityEHS solution.

27 M. J. O'Neil, *The Merck Index - An Encyclopedia of Chemicals, Drugs, and Biologicals. 13th Edition*, Whitehouse Station, NJ: Merck and Co., Inc., 2001.

28 E. Bingham, B. Cohrssen and C. H. Powell, *Patty's Toxicology Volumes 1-9 5th ed.*, John Wiley & Sons., New York, 2001.

29 R. J. Lewis, *Sax's Dangerous Properties of Industrial Materials. 11th Edition.*, Wiley ＆Sons，Inc, 2004.

30 European Chemicals Bureau; IUCLID Dataset http://esis.jrc.ec.europa.eu/, 2008.

31 T. R. Torkelson, S. E. Sadek and V. K. Rowe, Toxicologic investigations of 1,2-dibromo-3-chloropropane, *Toxicol. Appl. Pharm.*, 1961, **3**, 545-559.

32 R. J. Lewis, *Sax's Dangerous Properties of Industrial Materials. 9th ed. Volumes 1-3.*, Van Nostrand Reinhold, New York, 1996.

33 K. Nenpo, *Annual Report of Tokyo Metropolitan Research Laboratory of Public Health.*, toritsu Eisei Kenkyusho, Tokyo, 1972.

34 W. J. Hayes and E. R. Laws, *Handbook of Pesticide Toxicology. Volume 2. Classes of Pesticides*, Academic Press, Inc., 1991.

35 M. Hayyan, C. Y. Looi, A. Hayyan, W. F. Wong and M. A. Hashim, In Vitro and In Vivo Toxicity

Profiling of Ammonium-Based Deep Eutectic Solvents, *PLoS One*, 2015, **10**, e117934.

36 J. Chen, Q. Wang, M. Liu and L. Zhang, The effect of deep eutectic solvent on the pharmacokinetics of salvianolic acid B in rats and its acute toxicity test, *Journal of Chromatography B*, 2017, **1063**, 60-66.

37 P. de Morais, F. Gonçalves, J. A. P. Coutinho and S. P. M. Ventura, Ecotoxicity of Cholinium-Based Deep Eutectic Solvents, *ACS Sustain. Chem. Eng.*, 2015, **3**, 3398-3404.

38 NITE-CHRIP, Tokyo, Japan, Editon edn., 2015.

39 H. R. Rogers, Sources, behaviour and fate of organic contaminants during sewage treatment and in sewage sludges, *Sci. Total Environ.*, 1996, 3-26.

40 K. Urano and Z. Katz, Evaluation of biodegradation ranks of priority organic compounds, *Journal of hazardous materials*, 1986, **13**, 147-159.

41 T. Ishikawa, Y. Ose and T. Sato, Removal of organic acids by activated sludges, *Water Res.*, 1979, **13**, 681-685.

42 M. Dore, N. Brunet and B. Legube, Participation of Various Organic Compounds in the Evaluation of Global Pollution Criteria, *Trib Cebedeau*, 1975, **28**, 3-11.

43 G. W. Malaney and R. M. Gerhold, Structural determinants in the oxidation of aliphatic compounds by activated sludge, *J Water Pollut Control Fed*, 1969, **41**, R18-R33.

44 G. J. Nieme, Structural features associated with degradable and persistent chemicals, *Environ. Toxicol. Chem.*, 1987, **6**, 515-527.

45 G. W. Malaney and R. M. Gerhold, in *Proc 17th Ind Waste Conf.*, Purdue Univ, Editon edn., 1962, pp. 249-257.

46 Y. Yonezawa, *Kogai Shigen Kenkyusho Iho*, 1982, 85-91.